

Effect of Pore-Size Distribution on the Catalytic Performance for Coal Liquefaction. II. Carbonaceous and Metallic Deposition on the Catalyst

Hiromichi SHIMADA,* Minoru KURITA, Toshio SATO, Yuji YOSHIMURA,
Yoshinori KOBAYASHI, and Akio NISHIJIMA

National Chemical Laboratory for Industry, Yatabe, Ibaraki 305

(Received February 18, 1986)

The behavior of carbonaceous and metallic depositions on catalysts during hydroliquefaction of coal was investigated by using several kinds of catalyst supports with different pore-size distribution values in order to obtain the fundamental data for designing long-life catalysts. Higher concentration of carbonaceous deposition was observed on large-pore and bimodal catalysts than was observed on the comparative small-pore and unimodal catalysts, respectively. However, the carbonaceous deposit was distributed more evenly inside large pores than it was inside small pores. The micropores of the bimodal catalysts were more effectively used than were those of the unimodal catalysts. Thus, the unimodal catalysts with small pores suffered more severe pore-mouth poisoning than the bimodal or the large-pore catalysts. The penetration behavior of the metallic components was found to be different for each metal. Discrete minerals such as clay could not penetrate into the catalyst pores and were deposited on the external surface of the catalyst particle. While, the metallic components coordinated with organic compounds such as phenolates or chelates deposited inside the macro- and mesopores. Easy access of the large asphaltenic molecules to the active sites resulted in high coal-liquefaction activity for the catalyst. This was accompanied by large amounts of both carbonaceous and metallic depositions. It is concluded that large-pore or bimodal pore structure is required for both high liquefaction activity and suppression of pore-mouth poisoning.

In the previous paper,¹⁾ the authors reported that the pore-size distribution of the catalyst support have a great effect on the catalytic activity and selectivity for direct liquefaction of coal. The results are summarized as follows;

1. Catalysts with large pores are more advantageous in the production of asphaltenes (toluene-solubles) from coal than those with small pores.
2. Small pores tend to produce light products such as oils (hexane-solubles).
3. Bimodal catalysts with macroporosity ($r > 300$ nm) and microporosity ($r < 10$ nm) performed excellently in terms of both total liquefaction and oil production.

Another important catalytic performance required for hydrotreating catalysts, besides activity and selectivity, is long life time, which depends strongly upon carbonaceous deposition and metallic foulants on the catalyst. The recent development of catalysts for hydrotreating petroleum fractions has shown that it is necessary to clarify the behavior of the poisoning materials on the catalyst in order to design a new type of catalyst with longer life.^{2–7)}

Several investigations have been undertaken on the effects of the pore structure of the catalyst support on its aging behavior during hydroliquefaction of coal^{8,9)} or hydrotreating of coal-derived liquids.^{10,11)} They have demonstrated the beneficial effects of increasing pore radius or bimodal pore-size distribution of the catalyst support. As for the behavior of the carbonaceous and metallic foulants on the catalyst, it was found that there was a higher rate of deposition of the foulants during coal liquefaction as compared with petroleum hydroprocessing.

Bertolacini et al.⁸⁾ reported that the slowest decline of activity for hydroliquefaction of coal was found for bimodal catalyst with large micropores ($r \approx 10$ nm). They indicated that the surface area and pore volume decreased more rapidly for catalysts with small micropores than those with large pores. They also found that carbonaceous deposition caused a shift in micropore-size distribution with time on stream to lower pore diameter. Stiegel et al.¹⁰⁾ reported slower deactivation for catalysts with bimodal pore-size distribution than those with unimodal pores during hydrotreating of coal-derived liquids. They found that the former accumulates larger amounts of metallic foulants than the latter in spite of similar coke concentrations on all of the catalysts. Several researchers have applied electron microprobe (EPMA) analysis to the profiling of metallic components in catalyst particles and have reported different penetrations by the elements.^{12–14)}

In spite of these efforts, there still remain several questions unresolved concerning the aging behavior of catalysts because of the lack of information about the behavior of the poisoning materials on the catalyst. For example, it is still unclear why bimodal catalysts are much better than unimodal catalysts in terms of aging, although the superiority of the bimodal catalysts in the initial activity could be attributed to the high effective diffusivity.^{1,15,16)} It is not clear how each metallic foulant behaves on the catalyst and decreases the activity.

In the present paper, the authors aimed to clarify the behavior of foulants on catalysts in order to obtain the fundamental data needed for understanding the

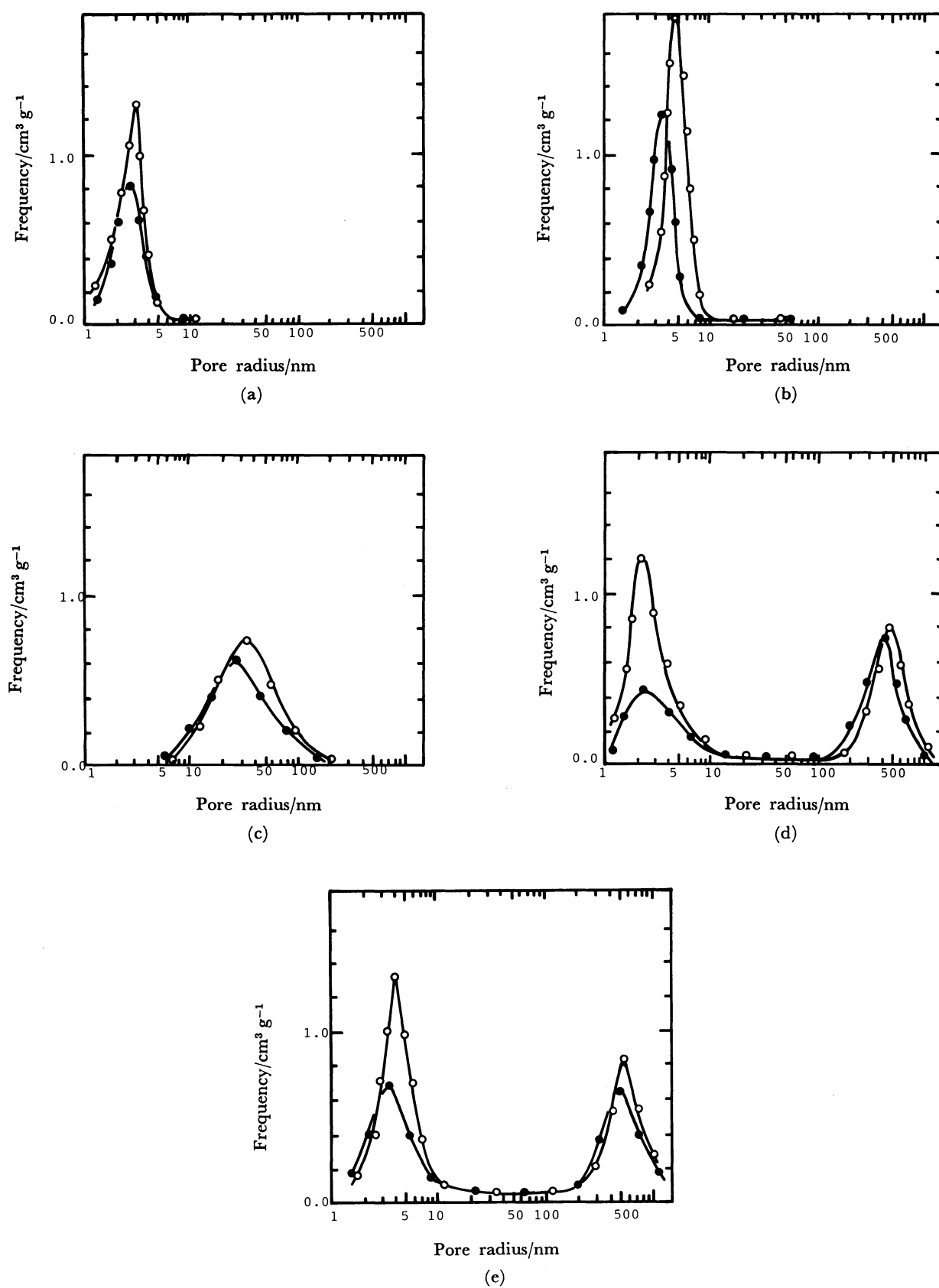


Fig. 1. Changes in pore-size distributions of the catalysts A (a), B (b), C (c), D (d), and E (e).
○: Fresh catalyst, ●: Used catalyst.

aging behavior of catalysts. Emphasis was placed on the effect of the pore structure on the deposition behavior. For this purpose, detailed analysis was carried out on five used catalysts with micro- ($r < 10$ nm), meso- ($10 < r < 100$ nm) and macroporosity ($r > 100$ nm) employing new surface analytical techniques such as X-ray photoelectron spectroscopy (XPS) and secondary ion mass spectrometry (SIMS) to investigate the metallic deposit.

Experimental

Catalysts. The molybdenum based catalysts were prepared by impregnation of Al_2O_3 supports (sphere with a diameter of 1.5 mm). The details of the procedures used are described in a previous paper.³⁾ The physical properties and chemical composition of the freshly prepared catalysts are summarized in Table 1. Pore-size distribution curves for the catalysts are shown in Fig. 1.

Reaction Procedure. The coal used was a subbituminous Taiheiyō coal containing 16.1% ash (dry base). All the reactions were carried out in a 500-cm³ autoclave with a magnetically-driven stirrer. The reaction conditions are as follows: hydrogen initial pressure (at 27 °C), 9.8 MPa; temperature, 400 °C; time, 2 h. Other details for procedures used are described in the previous paper.¹⁾

Characterization of the Catalyst. The catalyst used was Soxhlet extracted with tetrahydrofuran for 16 h and dried in vacuo at 300 °C before analysis. Analytical techniques

employed in this study of the fresh and used catalysts were as follows.

The carbonaceous deposit on the catalyst was determined by using a CHN analyzer (Yanagimoto, MT-3). A mercury porosimeter (AMINCO, 60000 psi) was used for the determination of the specific surface area, pore volume, and pore-size distribution of the catalyst. The amounts of Fe, Ca, and Ti deposited on the catalysts were measured by an X-ray fluorescence analyzer. An atomic absorption spectrometer was used in the determination of Na and Mg. An X-ray photoelectron spectrometer (XPS, Shimadzu ASIX-1000) with Mg anode (270 w) was used for evaluating the concentration of carbon and metallic elements on the surface of the catalyst particles.

A secondary ion mass spectrometer (SIMS, Hitachi IMA-2) was employed for the depth profiling of each metallic element around the external surface of the used catalyst. All the samples were bombarded by 10-keV O_2^+ ions at a current of about 2×10^{-6} A. A beam of electrons was applied to the sample's surface during analysis to prevent charge build-up.

Results and Discussion

Carbonaceous Materials. Table 1 shows the amount of carbon contained in the carbonaceous materials deposited on the catalyst during coal liquefaction. For unimodal catalysts, the carbon concentration on the surface of the catalyst increased with the pore radius of the catalyst support. This is in agreement with the trend observed for the catalysts used in hydrotreating petroleum residue.^{2,4)} This trend is attributed to the severe pore-diffusion limitation of the large molecules which cause carbonaceous deposition. It is also shown in Table 1 that carbonaceous materials were deposited in higher concentration on the bimodal catalysts (catalysts D and E) than they were on the unimodal catalysts (catalysts A and B). On the contrary, Stiegel et al.¹⁰⁾ reported that similar concentrations of carbon were deposited on both unimodal and bimodal catalysts during hydrotreating of coal-derived liquids. This discrepancy may be attributed to the difference in pore diffusion between coal and coal-derived liquids.

The changes in physical properties of the catalyst after coal liquefaction are also shown in Table 1. The $r(\text{S.A.})$ values (the ratio of the surface area of the used catalyst to that of the fresh one) increased with the pore radius, showing that the loss in the surface area was greater for small-pore catalysts than for large-pore catalysts. The bimodal catalysts (catalysts D and E) gave smaller $r(\text{S.A.})$ values than did the unimodal catalysts (catalysts A and B), again contrary to the results by Stiegel et al.¹⁰⁾, who reported similar concentration of carbon on both the catalysts. This discrepancy can be partly attributed to the fact that they chose bimodal catalysts with large micropores and unimodal catalysts with small micropores.

Figure 1 clearly shows the changes in pore-size distribution. Small micropores (Fig. 1 (a) and (d))

Table 1. Properties of the Fresh and the Used Catalysts

Catalyst	A	B	C	D	E
Fresh catalyst					
Phase of Al_2O_3 ^{a)}	γ	γ	α	γ	γ
S.A. ^{b)} /m ² g ⁻¹	276	211	39	316	261
P.V. ^{c)} /cm ³ g ⁻¹	0.37	0.48	0.55	0.76	0.84
MoO ₃ /wt%	3.4	3.2	2.8	3.5	2.9
Coal conversion activity					
TS ^{d)} yields/%	89.9	93.2	94.4	94.7	95.7
Used catalyst					
Carbonaceous deposition					
Carbon/wt% ^{e)}	6.9	6.7	2.0	10.7	10.1
Carbon/mg m ⁻² f)	0.25	0.32	0.51	0.34	0.39
Physical properties					
S.A./m ² g ⁻¹	175	199	41	147	180
$r(\text{S.A.})$ ^{g)}	0.63	0.94	1.0	0.47	0.69
P.V./cm ³ g ⁻¹	0.26	0.35	0.49	0.55	0.61
$r(\text{P.V.})$ ^{h)}	0.70	0.73	0.89	0.72	0.73

a) Decided by X-ray diffraction. b) Surface area. c) Pore volume. d) Asphaltene and oil (Toluene soluble). e) Calculated basing on the weight of fresh catalyst. f) Calculated basing on the surface area of the fresh catalyst. g) The ratio of the surface area for the used catalyst relative to that of the fresh one. h) The ratio of the pore volume for the used catalyst relative to that of the fresh one.

suffered severe pore plugging, while meso- and macroporosity did not change appreciably. More accumulated carbonaceous deposit was observed on the micropores of the bimodal catalysts than on those of the unimodal catalysts, which is consistent with Table 1.

It is clear that carbonaceous deposition is caused by large asphaltenic molecules, especially those containing heteroatoms such as nitrogen or oxygen.¹⁷⁾ Due to diffusion limitation of the large molecules, an increase in the concentration of the deposit was observed with increasing pore size. On the contrary, the smaller decrease in surface area and pore volume for the former than the latter indicated that the deposits were evenly distributed on the inner surface of large pores, while they localized around the mouth of the small pores (Fig. 2).

In the case of bimodal catalysts, the macroporosity enhanced the diffusion of large molecules into the micropores which are the branches between the macropores. The small pores of unimodal catalysts are narrow and long, while those of bimodal catalysts are connected to macropores, and are shallower (Fig. 2). Thus, the macroporosity caused a higher concentration of carbonaceous deposition on the inner surface of the micropores for the bimodal catalysts.

It has already been shown that most of the carbonaceous deposition on catalysts during the initial stage of a run is by reversibly adsorbed

molecules.^{2,18)} Therefore, high concentrations of reversibly adsorbed carbonaceous deposits on bimodal or large-pore catalysts during the initial stage of a run occurs on the inner surface of the catalyst and does not necessarily result in rapid deactivation of the catalyst. In fact, high total conversion was given over the large-pore catalyst, C, and the bimodal catalysts, D and E, (Table 1). It is apparent that the unimodal catalysts with microporosity suffered the most severe pore-mouth poisoning. It is important to prevent the production of inactive coke on the catalyst in order to reduce the deactivation rate of the catalyst. High pore diffusion may play an important role in the suppression of this production.

Metallic Foulants. Table 2 shows the amount of metallic foulants on the catalyst during coal liquefaction. In the table, the total amount deposited on each catalyst (5 g) is given. For each metallic component, the amount deposited increased with the pore radius of the catalyst support. The tendency was quite evident for Ca and Ti, but not as clear for Na.

Comparison of the amount of metal deposited on the catalyst with the total amount in coal showed that Ti and Mg were deposited on the large-pore catalysts preferentially. Little Si was deposited on the catalyst, although it was the most abundant metallic element in coal.

Table 3 shows the concentration, by XPS, of each metallic component on the external surface of the

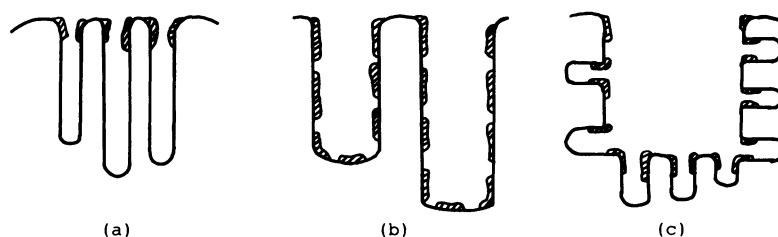



Fig. 2. Schematic diagram of pore structure of catalyst support and deposition behavior of carbonaceous materials (a): Small-pore catalyst (b): Large-pore catalyst (c): Bimodal catalyst : Carbonaceous materials.

Table 2. Deposited Metals^{a)} on the Used Catalysts

Catalyst	A	B	C	D	E	Coal ash ^{b)}
P.R. ^{c)} /nm	2.5	4.5	30	2.5, 350	4.5, 450	
Na ₂ O/mg	12	11	14	18	23	155
MgO/mg	4	3	9	11	14	61
CaO/mg	3	4	15	13	16	540
TiO ₂ /mg	1	4	7	11	17	83
Fe ₂ O ₃ /mg	5	7	13	16	17	500

a) The total amount deposited on all the catalyst (5 g). b) The total amount contained in the coal (60 g). Other major components are SiO₂ (6300 mg), Al₂O₃ (2000 mg), and K₂O (61 mg). The amount of SiO₂ and Al₂O₃ on the used catalyst could not be determined because they are the components of the fresh catalysts. The amount of K₂O was too little to be determined. c) Most probable pore radius.

catalyst. For all of the catalysts the XPS analysis gave a much higher concentration for each of the metallic foulants than was obtained by chemical analysis. It should be emphasized that very high concentrations of Ca, Ti, and Si were observed on the external surface layer, even for the small-pore catalysts (catalysts A and B), in spite of there being relatively little deposition through the entire catalyst particle.

The authors utilized a secondary ion mass spectrometer (SIMS) to investigate the penetration behavior of metallic foulants into the inner part of catalyst particles.^{19,20} SIMS analysis gave more detailed information on the profiling around the external surface of the particle as compared with EPMA. Figure 3 shows the depth-profile curves measured by SIMS. The ordinate, $I_{M\text{cor}}$ (corrected intensity for element M), is given by :

$$I_{M\text{cor}}(t) = \frac{I_M(t)/I_{Al}(t)}{I_M(0)/I_{Al}(0)},$$

Where $I_M(t)$ is the observed intensity for element M at sputtering time, t . The abscissa, sputtering time, is proportional to the depth from the external surface layer of the catalyst particle.

Figure 3 clearly displays the difference in the

Table 3. Deposited Metals on the External Surface of the Catalyst Sphere^{a)}

Catalyst	A	B	C	D	E
Na ₂ O/wt%	3.7	3.0	3.9	3.0	3.9
CaO/wt%	1.8	1.7	1.9	1.4	1.9
TiO ₂ /wt%	3.6	4.3	4.0	5.4	4.9
Fe ₂ O ₃ /wt%	4.5	3.3	4.9	3.0	2.1
SiO ₂ /wt%	23.	39.	18.	15.	34.

a) The determination was carried out by using XPS. And calculated basing on the measured area of the spectra and cross section given by Scofield.²¹⁾

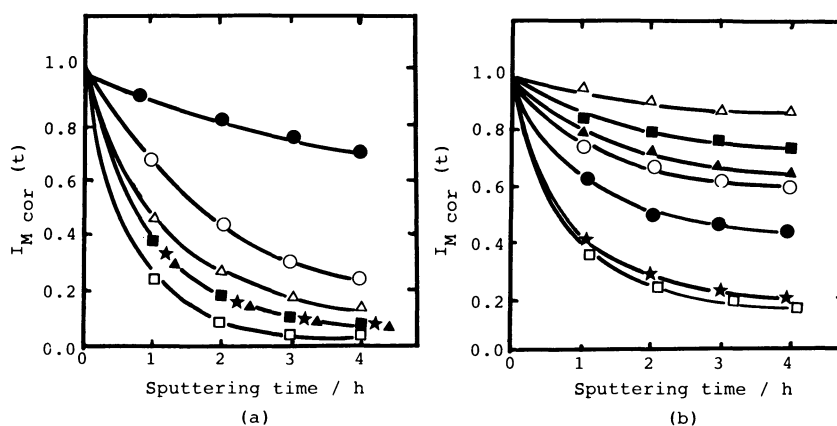


Fig. 3. Depth profiles of metal elements for the catalyst A (a) and the catalyst E (b).

●: Na, ○: Fe, △: Ca, ■: Mg, ★: Si, ▲: Ti, □: K.

behavior between the metallic elements. In the case of the small-pore catalyst A, Na showed much greater penetration than other elements. On the other hand, in the catalyst E with micro- and macropores, Ca, Mg, Ti, and Fe penetrated more deeply into the inner part of the catalyst particle than Na. For both catalysts, the profiles of Si and K decreased rapidly. Na could even penetrate into the catalyst particles having no large pores, while Ca, Ti, Fe, and Mg could not enter small pores. Si and K could not intrude even into large pores.

The above data, Tables 2, 3, and Fig. 3, clearly indicated that the metallic deposition behavior is quite different for each metal. The behavior of each metallic component is dependent upon its coordination which affects its effective particle size and its interaction with the catalyst. The metallic components can be classified into two categories.²²⁾ The first is as mineral matter present as discrete particles such as pyrite, quartz, and other clay minerals. The second is as organic matter which can be classified into two subcategories. One consists of inorganic salts of organic acids and the other as organic chelates.

The results indicate that most of the silicon in the coal occurs in the minerals, such as quartz, calcite, or kaolinite which could be observed as crystalline materials by X-ray diffraction. The particle size of the minerals is larger than the pore mouth of the macropores. High concentrations of Si on the external surface of the catalyst particles (Table 3) indicate the "filtration" of the minerals by the surface of the catalyst. It is inferred that most of the potassium occurs in the minerals also. This is in agreement with the results obtained by Gorin²²⁾ which indicated that K is an exception among alkali and alkaline earth metals.

Other elements, at least in part, will be associated with the organic matter. The major portion of the

alkali and alkaline earth metals in coal are present as inorganic salts of organic acids. The low pore-diffusion limitation seen for Na suggests that it is present as inorganic salts of low molecular weight organic acids such as phenols. Na from these phenolates was probably exchanged for protons from the acidic sites of the catalyst during deposition.

The next deepest penetration into the small-pore catalysts was observed for Fe (Fig. 3), which is consistent with the results in Table 2 that showed Fe was the second most abundant metallic foulant on small-pore catalysts. While, the ratio of the deposited amount to the total amount in coal was very low (Table 2). These results suggest that most of the iron is in the form of inorganic minerals, but that some of the iron is present in a small molecular weight component which can penetrate into catalyst pores. It cannot be excluded that a part of the iron is present as fine particles of minerals such as pyrite.

The low pore diffusion found for Mg and Ca indicated that these metals are present in large asphaltenic molecules, such as humates. Ca was deposited in a lower amount on the catalyst relative to the total amount in coal as compared with Mg (Table 2). This indicates that some of the Ca is present in minerals. The deposition behavior of Ti resembled that of Mg, indicating the presence of organotitanium chelate compounds.²²⁻²⁴⁾

Inorganic minerals are deposited on the external surface of the catalyst, which causes pore-mouth poisoning. More rapid deactivation of small particle size catalysts⁹⁾ can be attributed to this poisoning. Macroporosity of bimodal catalysts enhances the diffusion of large asphaltenic molecules into micropores, while it prevents the access of the minerals to the inner surface of the catalyst particle. The deposition of metals coordinated with organic compounds was caused by the decomposition of the organic matter. In fact, higher rate of metal deposition in the large-pore (catalyst C) or the bimodal (catalysts D and E) catalysts was accompanied by high coal-liquefaction activity of the catalyst (Table 1). As a consequence, it may be impossible to suppress the deposition without decreasing coal liquefaction activity. Therefore, high resistance against metallic deposition is required for catalysts with high activity and long life time.

As has been described above, the pore-size distribution greatly affects the deposition behavior of carbonaceous and metallic materials. On the large-pore and the bimodal catalysts, higher rates of deposition were observed than that found for the small-pore and the unimodal catalysts, respectively. However, deposition (except that due to inorganic minerals) results from the effective use of the inner surface of the catalyst which leads to high coal liquefaction activity. It was also found that large-pore or

bimodal catalysts are more advantageous than microporous unimodal catalysts from the view point of pore-mouth poisoning.

References

- 1) H. Shimada, M. Kurita, T. Sato, Y. Yoshimura, T. Kawakami, S. Yoshitomi, and A. Nishijima, *Bull. Chem. Soc. Jpn.*, **57**, 2000 (1984).
- 2) H. Beuther, O. A. Larson, and A. J. Perrotta, "The Mechanism of Coke Formation on Catalysts," in "Catalyst Deactivation," ed by B. Delmon and G. F. Froment, Elsevier, Amsterdam (1980), pp. 271-282.
- 3) S. T. Sie, "Catalyst Deactivation by Poisoning and Pore Plugging in Petroleum Processing," in "Catalyst Deactivation," ed by B. Delmon and G. F. Froment, Elsevier, Amsterdam (1980), pp. 545-569.
- 4) O. Togari, H. Takahashi, and M. Nakamura, *Sekiyu Gakkai Shi*, **23**, 256 (1980).
- 5) M. Nakamura, O. Togari, and T. Ono, Proc. Pan-Pacific Synfuels Conference, Tokyo, (1982), E-9.
- 6) K. Nomura, Y. Sekido, and Y. Ohguchi, *Sekiyu Gakkai Shi*, **23**, 321 (1980).
- 7) K. Nomura, Y. Sekido, and Y. Ohguchi, *Sekiyu Gakkai Shi* **24**, 253 (1981).
- 8) R. J. BertoLacini, L. C. Gutberlet, D. K. Kim, and K. K. Robinson, EPRI Report AF-1084 (1979).
- 9) L. M. Polinski, G. J. Stiegel, and R. E. Tischer, "1980 Status Review-Hydrolquefaction of Coal with Supported Catalysts," DOE/PETC/TR-81/2 (1981).
- 10) Y. Yoshimura, M. Kurita, T. Sato, H. Shimada, and A. Nishijima, *Kagaku Kogaku Ronbunshu*, **11**, 238 (1985).
- 11) G. J. Stiegel, R. E. Tischer, and L. M. Polinski, *Ind. Eng. Chem., Prod. Res. Dev.*, **22**, 411 (1983).
- 12) J. J. Stanulonis, B. C. Gates, and J. H. Olson, *AIChE J.*, **22**, 576 (1978).
- 13) T. L. Cable and F. E. Massoth, *Fuel Processing Technol.*, **4**, 265 (1981).
- 14) G. B. Freeman, B. D. Adkins, M. J. Moniz, and B. H. Davis, *Applied Catalysis*, **15**, 49 (1985).
- 15) L. M. Polinski, G. J. Stiegel, and L. Saroff, *Ind. Eng. Chem., Proc. Des. Dev.*, **21**, 477 (1982).
- 16) P. N. Ho and S. W. Weller, *Fuel Processing Technol.*, **4**, 21 (1981).
- 17) E. Furimsky, *Fuel Processing Technol.*, **6**, 1 (1982).
- 18) M. Ternan, E. Furimsky, and G. I. Parsons, *Fuel Processing Technol.*, **2**, 45 (1979).
- 19) H. Shimada, M. Kurita, T. Sato, Y. Kobayashi, Y. Yoshimura, and A. Nishijima, *Chem. Lett.*, **1983**, 181.
- 20) H. Shimada, Y. Kobayashi, M. Kurita, T. Sato, Y. Yoshimura, and A. Nishijima, Proc. 4th Int. Conf. on Secondary Ion Mass Spectrometry, Osaka (1983), p. 283.
- 21) J. H. Scofield, *J. Electron Spectrosc. Relat. Phenom.*, **8**, 129 (1976).
- 22) E. Gorin, "Fundamentals of Coal Liquefaction," in "Chemistry of Coal Utilization Second Supplementary Volume," ed by M. A. Elliot, John Wiley & Sons, New York (1981), p. 1904.
- 23) A. Robbat, Jr., D. H. Finseth, and R. G. Lett, *Fuel*, **63**, 1710 (1984).
- 24) R. Campo, H. J. Callot, P. Albrecht, and J. P. Kintzinger, *Tetrahedron Lett.*, **25**, 24 (1984).